Appl Microbiol Biotechnol (2003) 63: 115–127
DOI 10.1007/s00253-003-1432-2

MINI-REVIEW

N. Frankenberg · J. Moser · D. Jahn

Bacterial heme biosynthesis and its biotechnological application

Received: 23 June 2003 / Revised: 22 August 2003 / Accepted: 26 July 2003 / Published online: 16 September 2003

Abstract Proteins carrying a prosthetic heme group are vital parts of bacterial energy conserving and stress response systems. They also mediate complex enzymatic reactions and regulatory processes. Here, we review the multistep biosynthetic pathway of heme formation including the enzymes involved and reaction mechanisms. Potential biotechnological implications are discussed.

Introduction

Structure and function of tetrapyrroles

Compounds of the tetrapyrrole class are characterized by their four five-membered pyrrole rings, usually linked together via single atom bridges (Fig. 1). The four rings of the macrocycle are labelled clockwise A–D starting with the first of the three symmetric rings with regard to the ring substituents. Two classes of cyclic tetrapyrroles are found in nature. The porphyrins, including heme, bacteriochlorophyll and chlorophyll are characterized by their completely saturated ring system. The second class of more reduced cyclic tetrapyrroles, the porphinoids, includes vitamin B_{12} (corrinoids), siroheme, coenzyme F_{430} and heme d_1. In cyclic tetrapyrroles, the nitrogen atoms of the four pyrrole rings are used to chelate a variety of divalent cations. Tetrapyrroles are very distinct in color and amongst the most abundant molecules on earth. This is most visible in the green color of plants, which is due to their high chlorophyll content. In photosynthetic bacteria and plants, Mg-chelating chlorophylls and bacteriochlorophylls are the key pigments in trapping sunlight for photosynthesis (Beale 1999; Vavilin and Vermaas 2002).

N. Frankenberg (✉) · J. Moser · D. Jahn
Institute for Microbiology, Technical University of Braunschweig,
Spielmannstrasse 7,
38106 Braunschweig, Germany
e-mail: n.frankenberg@tu-bs.de
Tel.: +49-531-3915815
Fax: +49-531-3915854

The nickel-containing yellow coenzyme F_{430} is the prosthetic group of methyl-coenzyme M reductase that catalyzes the final step of methane formation in methanogenic archaea (Thauer and Bonacker 1994). The pink cobalt-containing vitamin B_{12} derivatives are the most complex known tetrapyrroles (Martens et al. 2002). They are involved in multiple enzymatic reactions, e.g., radical-dependent nucleotide reduction and methyl transfer. The iron-chelating yellow-greenish siroheme is required for the six electron transfer reactions during assimilatory nitrite or sulfite reduction (Raux et al. 2003). The green pigment heme d_1, is part of the dissimilatory nitrite reductase in Pseudomonads and is a typical porphinoid that differs significantly in structure and color from the other porphyrin-based hemes (Chang 1994).

The other commonly found tetrapyrrole structures are the open-chain molecules that are all derived from cleaved macrocycles. These can be divided into bile pigments, chlorophyll degradation products and phycobilins. The latter function as the direct chromophore precursor of the photoreceptor phytochrome and the cyanobacterial light-harvesting phycobiliproteins (for reviews see Hörtensteiner 1999; Frankenberg and Lagarias 2003). Although most linear tetrapyrroles are derived from heme by oxidative cleavage, their nomenclature is not consistent with that of the porphyrin system. The various rings of linear tetrapyrroles are also labelled A–D, but starting from the cleavage position of the heme macrocycle (Fig. 1).

In eukaryotes, the synthesis of tetrapyrroles is restricted to heme, siroheme, chlorophyll and bilins. Prokaryotes additionally form most complicated tetrapyrroles, such as corrinoids, heme d_1 and coenzyme F_{430} (Vavilin and Vermaas 2002).

Multiple physiological roles of heme

Heme, the iron-containing tetrapyrrole cofactor of hemoglobin is responsible for the red color of blood. In microorganisms, heme serves multiple cellular functions. As a prosthetic group of proteins it is involved, via its

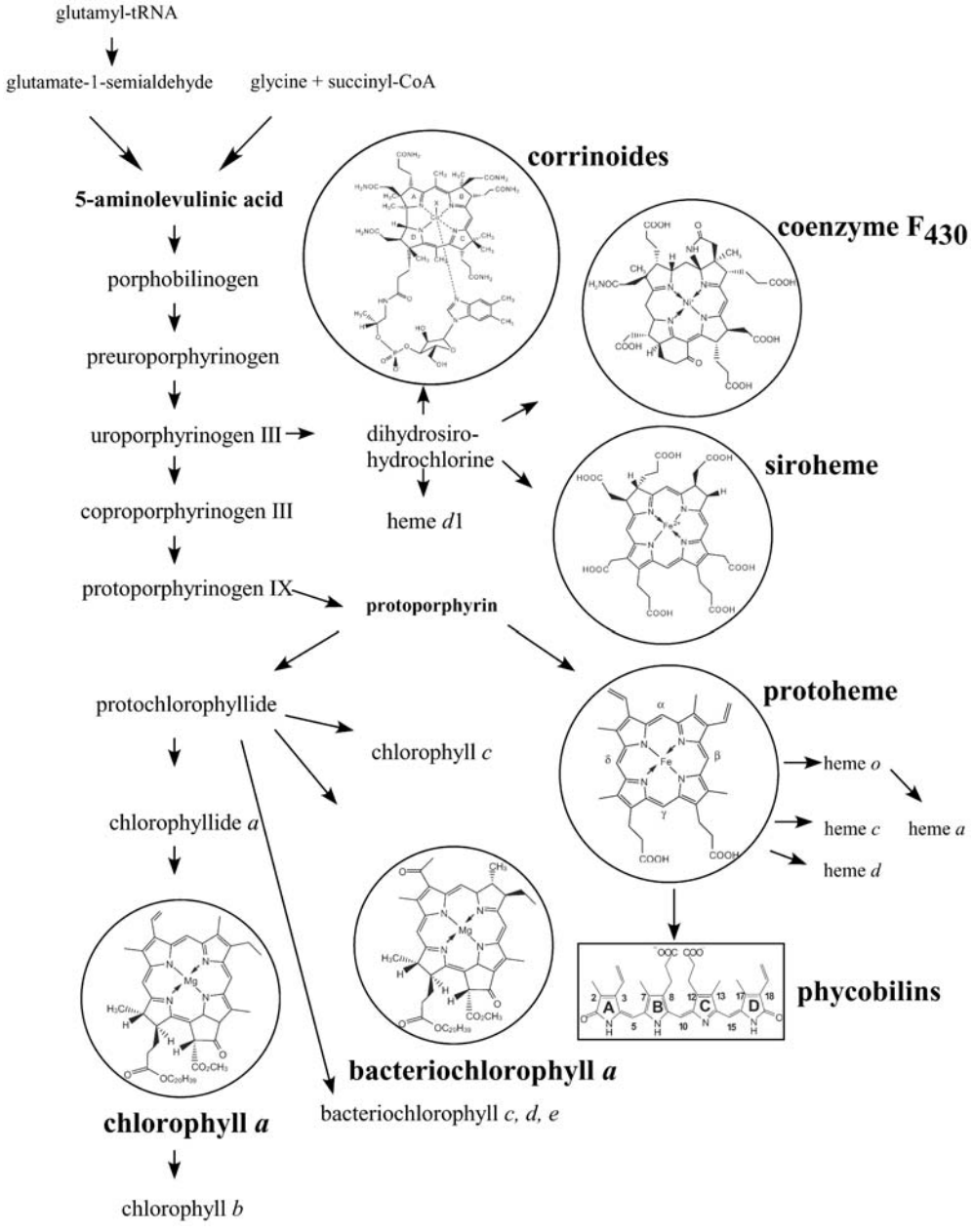

Fig. 1 Overview of the biosynthesis of tetrapyrroles in microorganisms. The six biologically important porphyrin- or porphinoid-based tetrapyrroles are shown in *circles*. Biliverdin IXα represents the group of linear tetrapyrroles (*box*)

electron transfer capacity, in the metabolism of molecular oxygen and diatomic gases and in multiple redox reactions. Exogenous heme can furthermore serve as an iron supply for pathogenic bacteria that colonize eukaryotic cells. On the other hand, heme acts as a regulatory molecule, modulating gene expression at the transcriptional and translational level. Furthermore, heme has been demonstrated to play a regulatory role in protein targeting, protein stability and cell differentiation (OBrian and Thöny-Meyer 2002; Schobert and Jahn 2002). In prokaryotes, cytochromes are the most abundant heme-containing proteins. Cytochromes are electron transfer proteins involved in the final reduction of oxygen in aerobic respiration. Interestingly, the requirement for heme is not restricted to aerobic metabolism. Anaerobic respiratory systems that employ alternative electron acceptors like nitrate also utilize electron transferring hemes (Zumft 1997). Thus, *Pseudomonas aeruginosa* has been shown to synthesize most of its heme under anaerobic denitrifying conditions (Schobert and Jahn 2002).

Figure 1 summarizes the biosynthesis of all known natural tetrapyrroles. In the following paragraphs we will specifically lead the reader through the biosynthesis of heme from simple precursors.

Two pathways for the biosynthesis of 5-aminolevulinic acid, the general precursor of all tetrapyrroles

The common precursor of all tetrapyrroles, 5-aminolevulinic acid (ALA) is synthesized in nature by two alternative, unrelated, routes called the C_5-pathway

(Beale and Castelfranco 1973; Jahn et al. 1992) and the Shemin pathway (Shemin and Russell 1953). The C_5-pathway, which is found in most bacteria, all archaea and plants, starts from the C_5-skeleton of glutamate and involves the subsequent action of two enzymes. The initial reduction of glutamyl-tRNA to glutamate-1-semialdehyde (GSA) is catalyzed by an NADPH-dependent glutamyl-tRNA reductase (GluTR). In the following reaction, glutamate-1-semialdehyde-2,1-aminomutase (GSAM) transaminates GSA in a pyridoxamine 5′-phos-

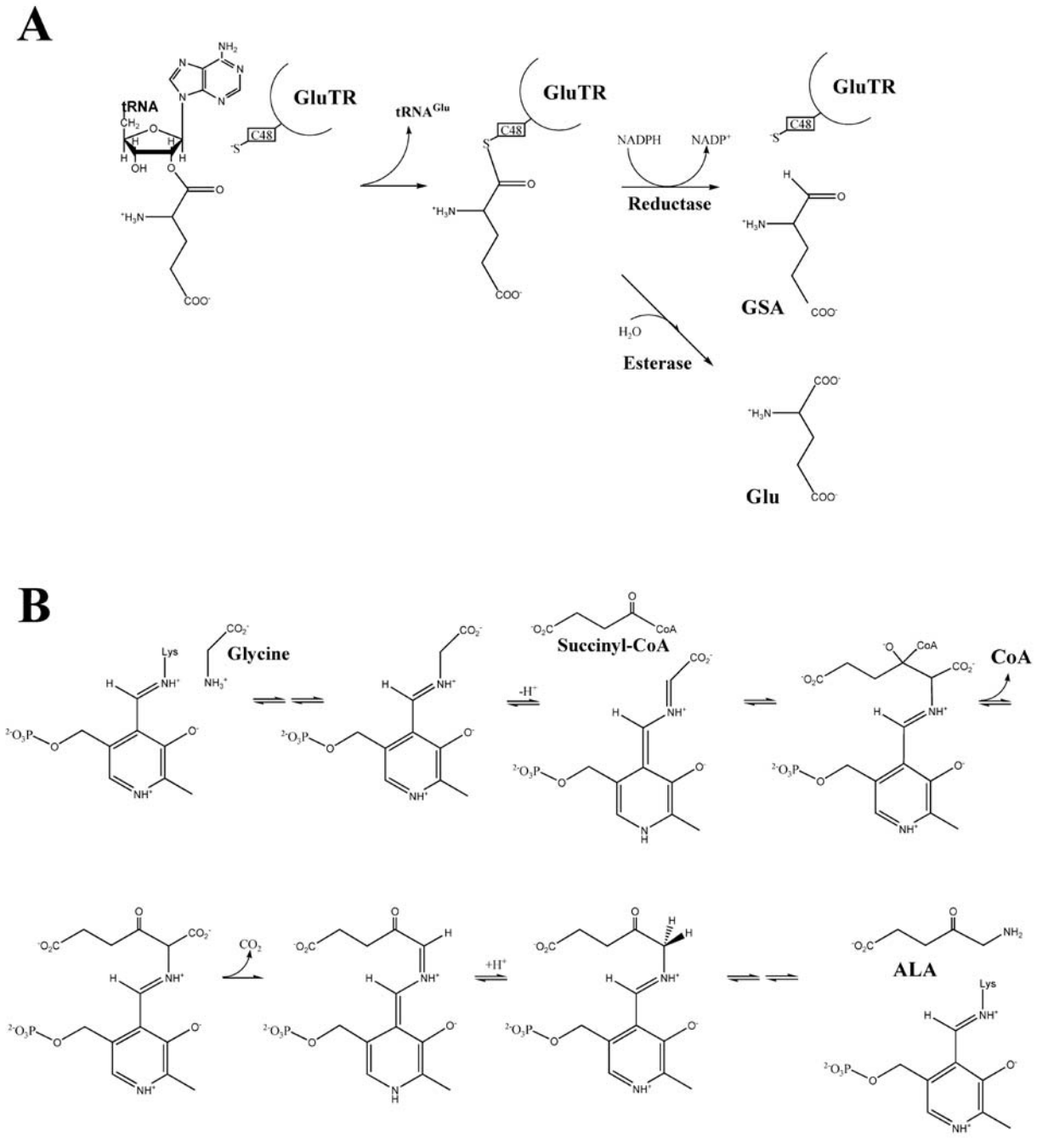

Fig. 2A, B Two routes for the biosynthesis of 5-aminolevulinic acid (ALA). **A** Thioester-dependent mechanism of glutamyl-tRNA-reductase (GluTR). The reactive cysteine residue nucleophilically attacks the aminoacyl bond of glutamyl-tRNA. An enzyme-localized thioester intermediate is formed with the release of free $tRNA^{Glu}$. The thioester is reduced by hydride transfer from NADPH leading to glutamate-1-semialdehyde (GSA). In the absence of NADPH the reactive thioester bond is hydrolyzed and glutamate is liberated. **B** Pyridoxal-5′-phosphate (PLP)-dependent mechanism of ALA synthase (ALAS). The reaction starts with a transaldimination leading to an external aldimine. After deprotonation, this aldimine is transferred into a transient chinonoid form reacting with succinyl-CoA. The CoA group is removed and an aldimine to α-amino-β-ketoadipate is formed. Upon cleavage of the C-α-carboxylate bond, CO_2 is released. A protonation at the C-5 position of the aldimine between PLP and the ALA formed then leads to dissociation of ALA

phate (PMP)-dependent reaction to form ALA (Jahn et al. 1992). In humans, animals, fungi and the α-group of proteobacteria, ALA synthase (ALAS) catalyzes the condensation of succinyl coenzyme A and glycine to ALA with the release of carbon dioxide and coenzyme A (CoA) (Gibson et al. 1958; Kikuchi et al. 1958). The only known example of an organism in which both pathways exist in parallel is the phytoflagellate *Euglena gracilis* (Weinstein and Beale 1983; Panek and OBrian 2002). In this organism both pathways are encoded by the nucleus but are translocated into different compartments: the C5 pathway into the chloroplast; ALAS into the mitochondria (Weinstein and Beale 1983).

Glutamyl-tRNA reductase

GluTR reductase is a very unique enzyme as its substrate is glutamyl-tRNA, which simultaneously participates in both protein and tetrapyrrole biosynthesis (ONeill and Söll 1990; Jahn et al. 1992). Aminoacylated $tRNA^{Glu}$ is reduced in an NADPH-dependent reaction to form GSA (Fig. 2A). Based on biochemical and crystallographic approaches using recombinant GluTR from the extreme thermophilic archaeon *Methanopyrus kandleri*, the catalytic mechanism and its structural basis have been established (Moser et al. 1999, 2001; Schubert et al. 2002b). Recently, the expression and purification of soluble *Escherichia coli* GluTR was enabled by the simultaneous co-expression of chaperones (Schauer et al. 2002, 2003). Treatment of *M. kandleri* and *E. coli* GluTR with iodoacetamide and 5,5′-dithiobis (2-nitrobenzoic acid) abolished enzyme activity indicating the involvement of a nucleophilic cysteine residue in catalysis. Mutagenesis studies identified the highly conserved residue Cys48 (*M. kandleri* numbering, Cys50 in *E. coli*) as the active site nucleophile. A catalytic mechanism for GluTR was proposed in which the sulfhydryl group of Cys48 (Cys50 in *E. coli*) nucleophilically attacks the α-carbonyl group of tRNA-bound glutamate forming an enzyme-bound thioester intermediate with concomitant release of $tRNA^{Glu}$ (Fig. 2A). This reaction intermediate has been isolated and visualized for *E. coli* GluTR (Schauer et al. 2002). Finally, hydride transfer from NADPH to the thioester-bound glutamate produces GSA. Surprisingly, both enzymes efficiently turned over glutamyl-tRNA in the absence of NADPH with release of glutamate. In this case a water molecule replaces NADPH, hydrolyzes the reactive thioester bond and liberates glutamate (Moser et al. 1999, 2001; Schauer et al. 2002). The crystal structure of *M. kandleri* GluTR has been solved and revealed an unusual extended V-shaped dimer (Fig. 3A, B) (Moser et al. 2001). Each monomer consists of three distinct domains, an N-terminal catalytical domain, an NADPH-binding domain and a C-terminal dimerization domain, arranged along an extended curved spinal α-helix (Fig. 3A, B). The crystal structure of GluTR was solved in complex with the competitive inhibitor glutamycin (Moser et al. 1999), representing the 3′-terminal adenosine residue of the tRNA where the bridging oxygen of the aminoacyl-group was replaced by nitrogen to form a stable amide bond. The structure of the enzyme-inhibitor complex supports the proposed catalytic mechanism (Moser et al. 1999, 2001; Schauer et al. 2002).

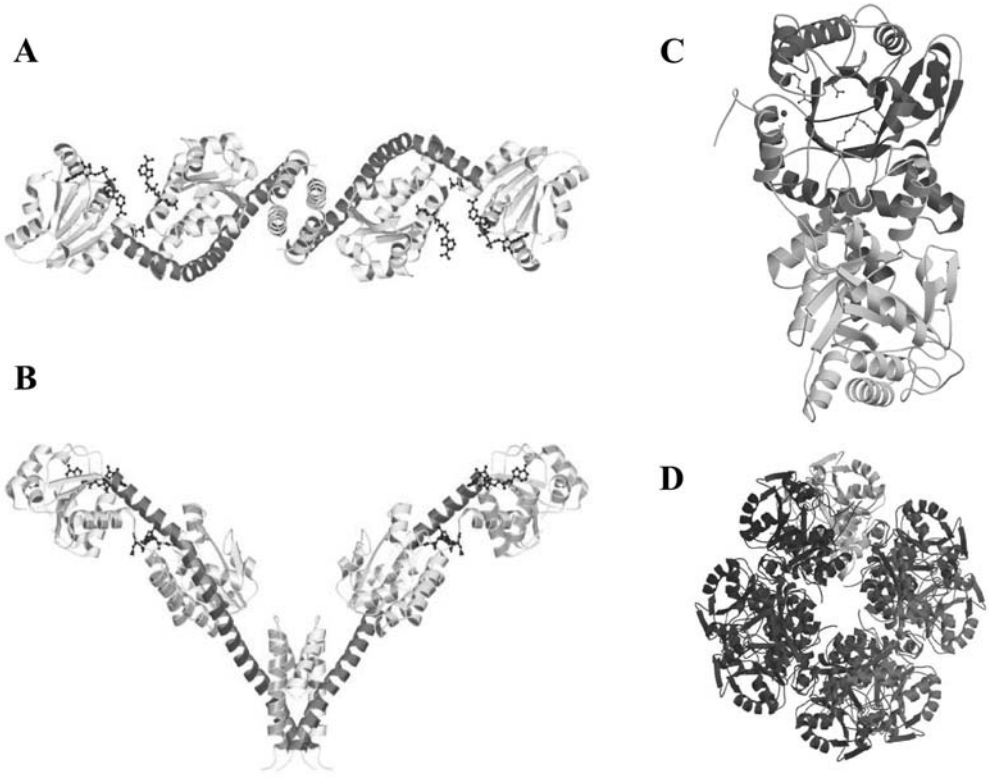

Fig. 3A–D Crystal structures of enzymes of the tetrapyrrole pathway. Schematic diagram of the *Methanopyrus kandleri* GluTR dimer viewed along the 2-fold-axis (**A**) and viewed perpendicular to the two-fold-axis (**B**). **C** Ribbon diagram showing the fold of the *Pseudomonas aeruginosa* porphobilinogen synthase (PBGS) dimer viewing towards the active site pocket of monomer A. **D** Structure of the PBGS octamer composed of four dimers projecting down the crystallographic 4-fold axis

Glutamate-1-semialdehyde-2,1-aminomutase

The second step of tRNA-dependent ALA formation requires the transfer of the C2 amino group of GSA to the C1 position. This reaction is catalyzed by pyridoxal 5′-phosphate (PLP)/PMP-dependent GSAM (E.C. 5.4.3.8), which is encoded by the *hemL* gene in bacteria (Jahn et al. 1992). The reaction differs from a classical aminotransferase reaction by its intramolecular nature. Nevertheless, GSAMs represent typical aminotransferases in catalysis and structure. Due to the nature of the PLP/PMP-cofactor of the enzyme, two catalytic paths are conceivable. Starting with the PLP form of GSAM, reaction with GSA results in the formation of dioxovalerate, while the PMP form leads to a 4,5-diaminovalerate (DAVA) intermediate. Recombinant GSAMs from *E. coli*, *Synechococcus* and other sources were found to catalyze both reactions (Smith et al. 1991b; Ilag and Jahn 1992). Intensive kinetic investigations of *Synechococcus* and pea GSAM eventually identified DAVA as the true intermediate and the PMP-dependent reaction as the relevant path (Smith et al. 1991a; Friedmann et al. 1992). GSAM catalyzes an anomalous enantiomeric reaction discriminating between (S)-GSA and (R)-GSA. Interestingly, (R)-GSA is a substrate for the first half-reaction but the resulting (R)-DAVA is either inactive or a poor substrate for the second half-reaction (Friedmann et al. 1992; Smith et al. 1992). GSAMs are inhibited by gabaculine, an inhibitor of gamma-aminobutyric acid transaminase and other aminotransferases. Additional inhibitors, 4-amino-hex-5-ynoate, 4-aminohex-5-enoate and enantiomers of diaminopropyl sulfate, have been developed (Tyacke et al. 1995; Contestabile et al. 2000b).

An active site lysine residue responsible for Schiff base formation with PMP was identified for various GSAMs (Grimm et al. 1992; Ilag and Jahn 1992). The three-dimensional structure of GSAM belongs to the extensively studied family of structurally related PLP-dependent proteins (Hennig et al. 1997). Besides aminotransferases, this class of enzymes includes mutases, synthetases, decarboxylases, and racemases. The dimeric protein has an overall ellipsoidal shape when viewed along the dimer axis. The monomers interact through a large, convoluted interface. Morphologically, no distinct domains are apparent. The PMP-cofactor and the substrate GSA are bound at the monomer-monomer interface. The crystal structure revealed the imperfect symmetry of the GSAM dimer. A loop consisting of residues 159–172 that is laterally covering the substrate pocket is partly disordered in one monomer, while it is well structured in the second. This loop is essential for proper enzyme function (Contestabile et al. 2000a). Presumably, GSAM oscillates between two conformational states in which one monomer is in the closed, active state (with ordered active-site lid), while the second is in a relaxed state, allowing product and substrate to diffuse out of and into the active site, respectively.

Metabolic channeling of GSA

The tRNA-dependent formation of ALA requires the coordinated action of GluTR and GSAM. Metabolically these enzymes are linked by the aldehyde GSA (Fig. 2A). Due to the chemical reactivity of GSA, solvent-exposed transfer of the highly reactive aldehyde from GluTR to GSAM seems unlikely. The complementary three-dimensional shape of GluTR and GSAM suggests an attractive solution to this metabolic problem (Moser et al. 2002). Placing the GSAM dimer from *Synechococcus* sp. (Hennig et al. 1997) alongside the extended, and similarly dimeric, GluTR immediately suggests that the open space delimited by the GluTR monomers could comfortably accommodate GSAM. The resulting model complex displays a striking degree of surface complementarity between both enzymes. The most convincing feature of the proposed GluTR/GSAM complex is that the putative active site entrance of each GSAM monomer is positioned opposite a depression in domain I of GluTR (Hennig et al. 1997). This depression and the glutamate recognition pocket of GluTR are separated only by Arg50 and are guarded by the conserved His84. The proposed complex may thus indicate that the GluTR-product GSA leaves the enzyme via the back door of the glutamate recognition pocket and directly channels to the active site of GSAM, a distance of about 26 Å, without being exposed to the aqueous environment (Moser et al. 2002).

5-aminolevulinic acid synthase

ALAS (EC 2.3.1.37) catalyzes the condensation of succinyl-CoA and glycine to produce ALA, carbon dioxide and free CoA. The enzyme is found in non-plant eukaryotes such as humans, animals and fungi. The α-group of the proteobacteria, including *Rhodobacter*, *Agrobacterium*, *Rhizobium* and *Rickettsia* species are the only prokaryotic representatives possessing ALAS (Avissar et al. 1989). ALAS contains a PLP cofactor and belongs to the α-oxoamine synthase subfamily of PLP-dependent enzymes. These enzymes typically catalyze the condensation of an amino acid and a carboxylic acid-CoA thioester in combination with the decarboxylation of the amino acid. ALAS is a functional homodimer in which residues of both subunits contribute to the active site. Based on the solved crystal structure of the closely related *E. coli* 8-amino-7-oxononaoate synthase, a model for the structure of *R. sphaeroides* ALAS was recently proposed (Alexeev et al. 1998). Here, a key residue for amino acid substrate recognition was identified (Shoolingin-Jordan et al. 2003).As in other PLP-dependent enzymes, catalysis starts with a transaldimination reaction between the substrate glycine and the internal aldimine formed between the aldehyde group of PLP and an active site lysine residue. After formation of the external aldimine, the *pro*-R proton of glycine is removed. The resulting transient quinonoid form is formed in the presence of the second substrate (Laghai and Jordan 1977; Nandi 1978;

Hunter and Ferreira 1999a, 1999b). During reaction of this quinonoid intermediate with succinyl-CoA, the CoA group is removed and an aldimine to α-amino-β-ketoadipate is formed. The quinonoid is then stabilized by the cleavage of the C-α-carboxylate bond. Protonation at the C-5 position of the aldimine between PLP and the ALA formed leads to the dissociation of ALA and ALAS (Hunter and Ferreira 1999b).

The first common step of tetrapyrrole biosynthesis: porphobilinogen synthase

The first step common to the biosynthesis of all tetrapyrroles is the asymmetric condensation of two molecules of ALA to form the monopyrrole porphobilinogen (PBG) (Fig. 1) (Shoolingin-Jordan et al. 2002). This reaction is catalyzed by porphobilinogen synthase (PBGS; aminolevulinic acid dehydratase; E.C. 4.2.1.24). PBGS

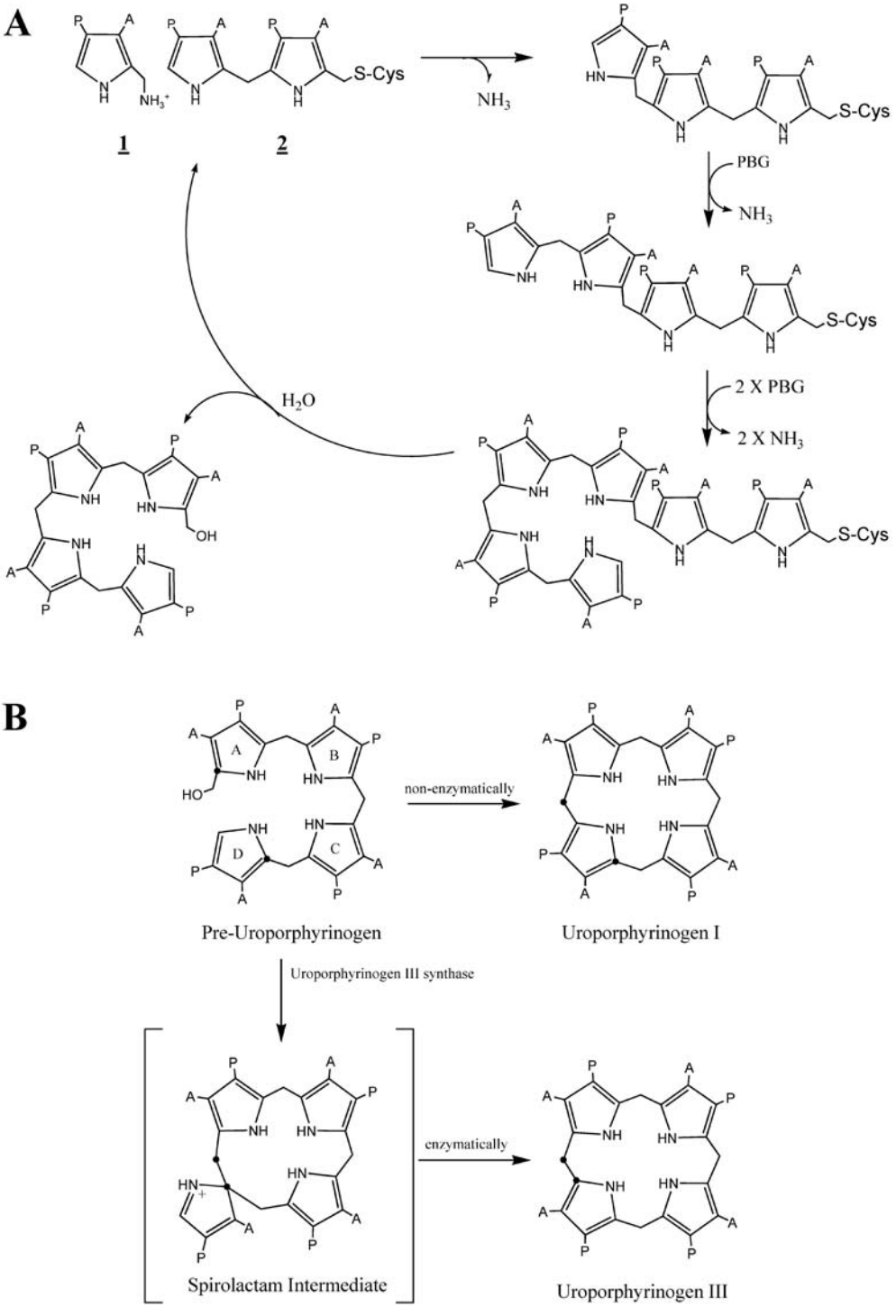

Fig. 4 Interesting enzyme mechanisms in heme biosynthesis. **A** Tetrapolymerization reaction catalyzed by porphobilinogen deaminase (PBGD). *1* Substrate PBG, *2*, dipyrromethane cofactor. The dipyrromethane cofactor is covalently attached to the protein via a cysteine residue. During each step one molecule of PBG is attached with the release of ammonia. The final product pre-uroporphyrinogen is hydrolytically released from the protein (see text for details). **B** Spiro-lactam intermediate in the biosynthesis of uroporphyrinogen III. Non-enzymatically pre-uroporphyrinogen is cyclized to the toxic uroporphyrinogen I. Uroporphyrinogen III synthase converts pre-uroporphyrinogen via an spirocyclic pyrrolene intermediate with inversion of the D ring to yield the asymmetric uroporphyrinogen III

enzymes are homo-octameric enzymes and highly variable in their cation dependence. The active site of PBGS contains two ALA binding sites designated A and P, according to the acetic acid and propionic acid side chains the ALA substrate contributes to the product PBG. The corresponding substrate molecules are consequently designated A- and P-side ALA. The formation of PBG involves the sequential formation of a C–C- and C–N-bond, respectively. The C–C-bond is formed by an aldol condensation whereas the C–N-bond is built by a Schiff-base. In the case of PBGS from the opportunistic pathogen *P. aeruginosa* it was shown that the synthesis of porphobilinogen involves a double Schiff-base mechanism. The reaction starts with binding of the P-side ALA, followed by A-side ALA binding. The removal of a hydrogen from C3 of the A-side ALA leads to the A-side enamine form. In the following step, a C–C-bond between the two ALA molecules is formed in an aldol-like addition. Through a Schiff-base exchange reaction, the C–N-bond between A- and P-side ALA is formed. After proton transfer and abstraction, the product is aromatized and released (Frere et al. 2002). All PBGS contain a metal-binding site at the active site that consists of either a cysteine-rich sequence (DXCXCX(Y/F)X_3G(H/Q)CG) or an aspartate-rich region (DXALDX(Y/F)X_3G(H/Q)DG. The cysteine-rich region is involved in zinc coordination. Enzymes that contain the aspartate-rich region do not use zinc but utilize magnesium and/or potassium instead. Besides the metal-binding region at the active site, many PBGS also contain an allosteric metal binding region ($RX_{\sim 164}DX_{\sim 65}EXXXD$) (Frankenberg et al. 1999b; Jaffe 2003). If present, the allosteric magnesium ion is involved in opening and closing a lid that covers the active site of each monomer (Frankenberg et al. 1999a). Since this complex metal-dependence has lead to some confusion in the literature in the past, a novel classification for PBGS enzymes has been proposed by Jaffe (2003). This new designation divides PBGS enzymes into four groups on the basis of an active site zinc and an allosteric magnesium ion.

Crystal structures of PBGS are available from human, yeast, *E. coli* and *P. aeruginosa* (Erskine et al. 1997, 1999; Frankenberg et al. 1999a). All structures are octameric and display the same overall fold. Each of the eight PBGS subunits consists of an $(\alpha\beta)_8$-barrel (Fig. 3C, D). One active site is located in each subunit and is close to the C-terminal end of the β-barrel. A flexible loop covers the active site and separates it from the surrounding medium. Also typical of all PBGS is an N-terminal extension that is involved in subunit-subunit interactions.

Porphobilinogen deaminase

The enzyme porphobilinogen deaminase (PBGD; hydroxymethylbilane synthase) (EC 4.3.1.8) catalyzes the stepwise polymerization of four molecules of PBG to the unstable linear tetrapyrrole, pre-uroporphyrinogen (1-hydroxymethylbilane). The tetramerization of PBG is catalyzed with the loss of four molecules of ammonia. During catalysis, the growing tetrapyrrole chain is covalently bound to the enzyme via a unique cofactor consisting of two molecules of PBG (Jordan and Warren 1987) (Fig. 4A). This dipyrromethane cofactor, itself covalently attached to the enzyme by a thioether linkage, acts as a primer in the tetramerization of PBG but is not enzymatically integrated into the final product. Figure 4A shows the polymerization reaction. One molecule of PBG is added per reaction cycle until an enzyme-bound hexapyrrole is formed. Each coupling step involves two sequential chemical reactions. First the substrate PBG is deaminated, followed by a nucleophilic attack by the α-carbon of the terminal ring of the enzyme-bound cofactor or the substrate cofactor-complex. Next, a hydrogen is removed from the α-position. The overall reaction is repeated four times. During the final step a water molecule attacks the tetrapyrrolic azafulvene to yield pre-uroporphyrinogen (Jordan 1994).

Several crystallographic structures of PBGD have previously been determined (Warren and Scott 1990; Hadener et al. 1993, 1999). The protein consists of three equal sized domains, the N-terminal, central- and C-terminal domains. The N-terminal and central domains depict similar topology: a modified parallel β-sheet. The C-terminal domain is an open-faced three-stranded sheet with one face covered by three α-helices. (Hadener et al. 1993). The volume of the active site cavity is designed to accommodate approximately 3½ pyrrole rings. This space limitation is responsible for the chain length and the final tetrapyrrolic product. PBGD is a monomeric enzyme and is encoded by the *hemC* gene. The product of the PBDG reaction, pre-uroporphyrinogen is very unstable and will autocatalytically cyclize to the toxic uroporphyrinogen I. Intermediates derived from this completely symmetric molecule inhibit enzymes of the pathway that require asymmetry for substrate recognition. Therefore, the presence of the next enzyme in the pathway, uroporphyrinogen III synthase prevents the release and solvent exposure of pre-uroporphyrinogen.

Uroporphyrinogen III synthase

Uroporhyrinogen III synthase (Cosynthase; E.C. 4.2.1.75) is a small enzyme that catalyzes the cyclization of pre-uroporphyrinogen with the inversion of ring D to the first asymmetric molecule in the pathway, uroporphyrinogen III (Fig. 4B). Mechanistic studies have shown that the formation of uroporphyrinogen III involves an electrophilic addition of the substrates hydroxymethyl group to C-16, which subsequently results in the cleavage of the C-15 to C-16 bond. This mechanism is referred to as the spiro-mechanism since the key intermediate is a spiropyrrolenine produced by the initial cyclization (Fig. 4B). This mechanism is supported by the strong inhibition caused by a spiro-lactam intermediate homologue. The amino acid sequences of uroporhyrinogen III synthases from different organisms show little if any homology. Most of the conserved amino acid residues are located in a

large open cleft that is positioned between two central domains. This region of uroporhyrinogen III synthase seems to accommodate the active site (Mathews et al. 2001). The two central domains fold into a parallel β-sheet surrounded by α-helices that are connected via a β-ladder. The structure provides clear evidence for interdomain flexibility. This suggests that a considerable conformational change may be required during catalysis (Mathews et al. 2001; Schubert et al. 2002a).

Uroporphyrinogen decarboxylase

Uroporphyrinogen decarboxylase (URO-D; E.C.4.1.1.37) catalyzes the sequential decarboxylation of the four acetate side chains of uroporphyrinogen III, localized at C-2, C-7, C-12 and C-18, to yield methyl groups with the formation of coproporphyrinogen III (Akhtar 1991). URO-D is a homodimeric protein consisting of two subunits that fold into a distorted $(\alpha\beta)_8$-barrel (Whitby et al. 1998; Martins et al. 2001). URO-D appears to be the first known decarboxylating enzyme with no requirement for a cofactor or prosthetic group (de Verneuil et al. 1983). At physiological substrate concentrations, decarboxylation occurs in an ordered manner, starting with the acetate side chain of the asymmetric ring (ring D). Interestingly, under excess substrate concentrations the reaction seems to occur randomly (Luo and Lim 1993). It has been proposed that the protonated pyrrole ring serves as an electron sink that promotes electron withdrawal (Akhtar 1991). Although crystal structures of the enzyme are available (Whitby et al. 1998; Martins et al. 2001), there is still a great lack of understanding of the exact catalytic mechanisms. The reaction is especially intriguing as a 180° flip of the first reaction intermediate is required to bring the side chains of ring A into the active site that was previously occupied with the side chains of ring D. A dimer-dependent mechanism has been proposed in which the rate-limiting decarboxylation of ring D occurs at the active site of one monomer while the other three decarboxylations may take place at the catalytic cleft of the other monomer (Martins et al. 2001).

Coproporphyrinogen III oxidases

The oxidative decarboxylation of coproporphyrinogen III (coprogen) to protoporphyrinogen IX (protogen) is catalyzed by different types of coproporphyrinogen III oxidases (CPO, EC 1.3.3.3). CPO consecutively converts the propionate side chains of rings A and B to their corresponding vinyl groups (Akhtar 1991). Molecular oxygen serves as the electron acceptor for the oxidative decarboxylation reaction under aerobic conditions. In the absence of oxygen, alternative electron acceptors are utilized for catalysis. Therefore, at least two different types of enzymes for coprogen oxidation are found in nature, one for the oxygen-dependent (HemF) and another for the oxygen-independent reaction (HemN, HemZ).

Oxygen-dependent coproporphyrinogen III oxidase HemF

Most available data on oxygen-dependent CPO (E.C. 1.3.3.3) are for enzymes from eukaryotic sources. In mammals, the protein is found associated with the inner side of the mitochondrial outer membrane. However, the enzyme was also found in the cytosol of *Saccharomyces cerevisiae* (Dailey 2002). Human oxygen-dependent CPO is a dimer of identical subunits with no detectable metal ions or cofactors. Nevertheless, molecular oxygen is required for catalysis (Medlock and Dailey 1996). Recently, a structural model for CPO based on the structure of urate oxidase has been proposed (Colloch et al. 2002). Both enzymes are similar with regard to the catalytically required molecular oxygen and the observed lack of detectable cofactors or metal ion (Colloch et al. 2002). Urate oxidase, which is involved in purine degradation, depicts a so-called tunneling-fold (T-fold), composed of four sequential β-strands with a pair of antiparallel α-helices between the second and third strand. In general, proteins that carry a T-fold are structurally very similar while their amino acid sequence homology is very low.

Oxygen-independent CPOs: HemN and HemZ

Until recently, much less was known about the oxygen-independent CPO that is encoded by the *hemN* gene. Some bacteria carry a second *hemN*-like gene termed *hemZ*. The gene product shows significant amino acid sequence homology to HemN and was shown to be involved in oxygen-independent coproporphyrinogen III oxidation (Homuth et al. 1999). There are no obvious similarities at the amino acid sequence level between oxygen-dependent HemF and the oxygen-independent CPOs HemN and HemZ. Anaerobically purified HemN is a monomeric protein with a native M_r of 52,000±5,000 Da. The enzyme requires S-adenosylmethionine (SAM) and both an electron-donor and -acceptor for catalysis. Furthermore, an oxygen-sensitive [4Fe-4S]-cluster was identified by absorption spectroscopy and iron analysis (Layer et al. 2002). The cysteine residues C62, C66, and C69, which are part of a conserved CXXXCXXC motif found in all HemN proteins, are essential for iron-sulfur cluster formation and enzyme function. The observed functional properties, in combination with a recently published computer-based enzyme classification, identified HemN as a Radical SAM enzyme (Sofia et al. 2001; Layer et al. 2002). Hence, a radical mechanism for the oxidative decarboxylation of coproporphyrinogen III by HemN has recently been postulated (Fig. 5) (Layer et al. 2002). This mechanism involves the reduction of the [4Fe-4S]-cluster from the +2 to the +1 state followed by an electron transfer to SAM and the homolytic cleavage of SAM to methionine and a 5′-deoxyadenosyl radical. This radical abstracts a hydrogen atom from the β-C atom of the propionate side chain of the substrate and generates the corresponding

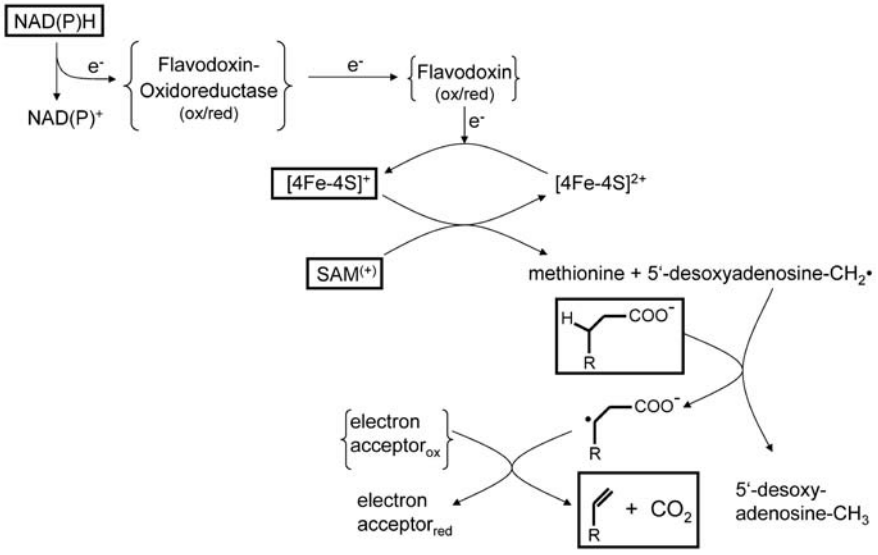

Fig. 5 Postulated radical mechanism of oxygen independent coproporphyrinogen III oxidase (CPO). The homolytic cleavage of S-adenosylmethionine (SAM) generates a 5′-deoxyadenosyl radical that subsequently abstracts a hydrogen atom from the propoinate side chain of the substrate to yield 5′-deoxyadenosine and a substrate radical. The electron donor for this step is the enzymes $[4Fe\text{-}4S]^+$ cluster. In the next step, the vinyl group of the product is formed through the elimination of CO_2. This step requires an electron acceptor to collect the remaining electron of the substrate radical (Layer et al. 2002). *Boxed* compounds represent identified components, whereas compounds *in brackets* represent activities still unknown

substrate radical. During the final reaction step the vinyl group is formed and CO_2 is released. This last step requires an electron acceptor whose nature remains to be identified (Fig. 5).

Protoporphyrinogen IX oxidase

Protoporphyrinogen IX oxidase (PPO; E.C. 1.3.3.4) catalyzes the six electron oxidation of protoporphyrinogen IX to form protoporphyrin IX. The result of this oxidation reaction is a conjugated double system of the tetrapyrrole macrocycle. Best characterized are the PPOs from eukaryotes, where the enzyme is located on the cytosolic side of the inner mitochondrial membrane. Molecular oxygen serves as the terminal electron acceptor. Plant-type PPOs are sensitive to diphenyl ether herbicides (e.g., acifluorfen-methyl), which inhibit the enzyme leading to the accumulation of protoporphyrinogen (Arnould and Camadro 1998). Protoporphyrinogen subsequently diffuses out of the mitochondria where it is non-enzymatically oxidized to the phototoxic protoporphyrin.

Protoporphyrinogen oxidation in prokaryotes is far from being understood. Three different genes encoding putative bacterial PPOs have been described during recent decades: *hemG*, *hemK* and *hemY* (Panek and OBrian 2002). *E. coli hemK* was originally identified in a genetic screen for heme biosynthetic mutants. It was suggested that *hemK* might be a subunit of a larger multienzyme complex catalyzing the conversion of protoporphyrinogen IX to protoporphyrin IX. However, it was subsequently determined that the *hemK* gene product does not contribute to PPO activity. Later HemK was biochemically identified as a methyltransferase (Heurgue-Hamard et al. 2002). The *E. coli hemG* gene was first identified by Sasarman and coworkers by the accumulation of protoporphyrinogen by an appropriate *hemG* mutant. The heme auxotrophic phenotype was rescued by expression of *hemG* or a eukaryotic PPO gene in trans (Sasarman et al. 1979, 1993). Until now, no direct biochemical data have been obtained for the proposed PPO function. So far, *hemG* genes are limited to six genera within the γ-group of proteobacteria and to *Mesorhizobium loti*, an α-group proteobacterium. The *hemG* gene might be unique to these few bacteria, contributing to a larger multienzyme complex in a species-specific manner (OBrian and Thöny-Meyer 2002).

In the Gram-positive soil bacterium *Bacillus subtilis* the *hemY* gene encodes a PPO that is similar to the eukaryotic enzyme. HemY contains a flavin cofactor and utilizes molecular oxygen as a terminal electron acceptor (Hansson and Hederstedt 1994). The *Bacillus* protein is a soluble monomer with a relative molecular mass of 50,000 Da (Dailey 2002). Interestingly, the *Bacillus* HemY enzyme is resistant to diphenyl-herbicides as are transgenic plants expressing the *B. subtilis hemY* gene (Lee et al. 2000). On the other hand, the *hemY* gene product from the Gram-negative *Myxococcus xanthus* is sensitive to this type of herbicide (Dailey 2002).

In general, *hemG* or *hemY* genes are not usually found in heme-synthesizing prokaryotes. Among 28 heme synthesizing genera, 14 do not contain a recognizable PPO gene (*hemG* or *hemY*) (Panek and OBrian 2002). Even well studied organisms like *P. aeruginosa* and photosynthetic cyanobacteria like *Synechocystis* sp. PCC6803 do not contain *hemY* or *hemG* homologues. These observations imply that a so far unknown locus encodes a novel type of protoporphyrinogen oxidase.

Alternatively, an already known protein might carry an additional enzymatic activity. One candidate is the PPO from the anaerobic bacterium *Desulfovibrio gigas* (Klemm and Barton 1987). The chromatographically purified enzyme was found to be composed of three dissimilar subunits and used 2,6-dichlorophenol-indophenol as an alternative electron acceptor.

Ferrochelatase

The last enzymatic step of heme biosynthesis is the insertion of iron into the tetrapyrrole macrocycle of protoporphyrin IX . This reaction is catalyzed by ferrochelatase (E.C. 4.99.1.1; protoheme ferrolyase). The three-dimensional structure of the membrane-associated human ferrochelatase reveals a homodimeric protein containing two [2Fe-2S] clusters (Wu et al. 2001).

One of the most intensively studied ferrochelatases originates from *B. subtilis* and is encoded by the *hemH* gene. The three-dimensional structure of the monomeric enzyme has been determined at a resolution of 1.8 Å (Al-Karadaghi et al. 1997). The ferrochelatase consists of two similar domains each with a four-parallel β-sheet flanked by α-helices. The active site is formed by elements protruding from both domains as a deep cleft. The structure of ferrochelatase, in complex with the competitive inhibitor *N*-methyl mesoporphyrin IX and the artificial product Cu-mesoporphyrin IX, has provided insight into the enzymatic mechanism of porphyrin metallation (Lecerof et al. 2000). The data obtained support a mechanism in which the pyrrole rings B, C and D are fixed by ferrochelatase in a vice-like grip while ring A is forced into a 35° tilted conformation. The metal ion enters the porphyrin via this tilted ring A after pyrrole proton abstraction mediated by a conserved histidine residue.

Potential biotechnological applications of heme biosynthesis

Cancer phototherapy and understanding of porphyrias

Porphyrins generate reactive oxygen species when excited by light, which can lead to cell death. Today this phototoxic effect is utilized for cancer therapy. The application of the heme precursor ALA to tumor cells is a common approach to induce the required porphyrin accumulation (Fuchs et al. 2000). This exogenous administration of ALA bypasses the several heme-dependent autoregulatory steps and results in a significant accumulation of photoexcitable protoporphyrin IX (Malik and Lugaci 1987). Protoporphyrin IX is, however, rapidly converted to heme by ferrochelatase in the presence of iron. Therefore, insight into the molecular basis of ferrochelatase catalysis and the design of useful inhibitors could lead to improvements in clinical photodynamic therapy of cancer. The ALA employed is of bacterial origin. Photosynthetic bacteria like *Rhodobacter spaeroides* JFO 12203 have been successfully used for the production of ALA. If grown on culture medium containing levulinic acid, an inhibitor of PBGS, the next enzyme in the pathway, this bacterium is an effective producer of ALA (Bykhovskii et al. 1998).

Porphyrias are inherited or acquired disorders in the heme biosynthetic pathway (Elder 1998). Heme (iron-protoporphyrin IX) formation is blocked at various steps, which leads to an excess excretion of porphyrin or porphyrin precursors—hence the term porphyria. According to current classification, porphyrias are divided in two main groups: the acute porphyrias and nonacute porphyrias. Acute porphyrias attract most attention, because they can be accompanied by life-threatening porphyric attacks. An understanding of the detailed molecular function of various heme biosynthetic enzymes provides the basis for rational drug design in order to sustain photodynamic phototherapy and tackle the various inherited porphyrias. However, many of the eukaryotic enzymes involved are difficult to explore by the required biochemical and biophysical methods due to their resistance to recombinant technologies and their often membrane-associated character. Their highly homologous prokaryote counterparts, however, provide a useful tool for fundamental basic and applied research.

Antioxidants and cytotoxic compounds

Recent data reveal that an inducible hemeoxygenase is upregulated in peripheral ganglia after axonal injury. This observation suggests a role for the reaction product carbon monoxide in cellular signaling and a requirement for the antioxidants biliverdin and bilirubin during the regeneration process (Magnusson et al. 2000). Manipulation of hemeoxygenase expression could proof a useful tool for brain injury therapy.

Novel tetrapyrroles have been isolated from the marine cyanobacterium *Tolypothrix nodosa*. Tolyporphin, an atypical tetrapyrrole, belongs to the class of bacteriochlorins (Montforts and Glasenapp-Breiling 2002). Again, this novel compound carries significant cytotoxic activity. Therefore, its potential use in anticancer therapy is thinkable (Bykhovskii et al. 1998).

Vitamin B_{12} production

One major tetrapyrrolic product generated by biotechnological processes using bacteria is vitamin B_{12} (for details, see review by Martens et al. 2002). The initial, partly rate-limiting, four or five steps of vitamin B_{12} synthesis are common to those of heme formation. Recently, it was shown that overexpression of the genes involved in combination with protein engineering approaches aimed at the initial enzyme greatly enhance vitamin B_{12} production (H. Barg, J.H. Martens, D. Jahn, unpublished data).

Overexpression of heme biosynthesis genes to increase the yield of commercial peroxidases

Peroxidases are heme-containing enzymes that utilize hydrogen peroxide or other peroxides to catalyze the free-radical-mediated oxidation of a variety of organic and inorganic compounds. Microbial and many fungal peroxidases are involved in the degradation of lignin and other phenolic compounds. Peroxidases are also used for bioremediation strategies or as additives to detergents and personal care products. Hydrogen peroxide is also used for the disinfection of contact lenses. The residual hydrogen peroxide after disinfections can be removed by a heme-containing catalase that converts hydrogen peroxide into water and oxygen.

In order to increase the production of recombinant fungal peroxidases/catalases, genes encoding the first enzymes of the heme biosynthesis pathway from *Aspergillus oryzae* were overexpressed. It was shown that integration of multiple copies of the *hemA* gene encoding ALA synthase, under the transcriptional control of the inducible TAKA promoter, into the chromosome of *A. oryzae* resulted in a 2-fold increase in heterologous peroxidase production.

Novel antibiotic targets

Since the initial steps of heme biosynthesis differ between human (ALA synthase) and most bacteria (GluTR), novel inhibitors with antimicrobial activity can be developed. In agreement with this approach it was shown for *Salmonella* that strains carrying a defective *hemA* gene for GluTR had reduced infection capacity (Benjamin et al. 1991).

Phycobiliproteins as fluorescent markers in cell biology

The linear tetrapyrrole-containing phycobiliproteins of cyanobacteria and red algae are involved in light harvesting and energy transfer reactions. Thus, phycobiliproteins exhibit not only strong absorption properties but are also highly fluorescent (Sidler 1994). This property has provided a helpful tool for cell biology. Phycobiliprotein-labeled detection reagents have been used extensively in flow cytometry to detect cell-specific expression of surface antigens.

Acknowledgements Research in the authors laboratory was supported by funds from the Deutsche Forschungsgemeinschaft und the Fonds der Chemischen Industrie.

References

Akhtar M (1991) Mechanism and stereochemistry of the enzymes involved in the conversion of uroporphyrinogen III into haem. In: Jordan PM (ed) Biosynthesis of tetrapyrroles. Elsevier, Amsterdam, pp 67–99

Alexeev D, Alexeeva M, Baxter RL, Campopiano DJ, Webster SP, Sawyer L (1998) The crystal structure of 8-amino-7-oxononanoate synthase: a bacterial PLP-dependent, acyl-CoA-condensing enzyme. J Mol Biol 284:401–419

Al-Karadaghi S, Hansson M, Nikonov S, Jonsson B, Hederstedt L (1997) Crystal structure of ferrochelatase: the terminal enzyme in heme biosynthesis. Structure 5:1501–1510

Arnould S, Camadro J-M (1998) The domain structure of protoporphyrinogen oxidase, the molecular target of diphenyl ether-type herbicides. Proc Natl Acad Sci USA 95:10553–10558

Avissar YJ, Ormerod JG, Beale SI (1989) Distribution of delta-aminolevulinic acid biosynthetic pathways among phototrophic bacterial groups. Arch Microbiol 151:513–519

Beale SI (1999) Enzymes of chlorophyll biosynthesis. Photosynth Res 60:43–73

Beale SI, Castelfranco PA (1973) ^{14}C incorporation from exogenous compounds into δ-aminolevulinic acid by greening cucumber cotyledons. Biochem Biophys Res Commun 52:143–149

Benjamin WH Jr, Hall P, Briles DE (1991) A *hemA* mutation renders *Salmonella typhimurium* avirulent in mice, yet capable of eliciting protection against intravenous infection with *S. typhimurium*. Microb Pathog 11:289–295

Bykhovskii V, Zaitseva NI, Eliseev AA (1998) Tetrapyrroles: diversity, biosynthesis, biotechnology. Appl Biochem Microbiol 34:1–18

Chang CK (1994) Haem d1 and other haem cofactors from bacteria. Ciba Found Symp 180:228—246

Colloch N, Mornon JP, Camadro JM (2002) Towards a new T-fold protein?: the coproporphyrinogen III oxidase sequence matches many structural features from urate oxidase. FEBS Lett 526:5–10

Contestabile R, Angelaccio S, Maytum R, Bossa F, John RA (2000a) The contribution of a conformationally mobile, active site loop to the reaction catalyzed by glutamate semialdehyde aminomutase. J Biol Chem 275:3879–3886

Contestabile R, Jenn T, Akhtar M, Gani D, John RA (2000b) Reactions of glutamate 1-semialdehyde aminomutase with R- and S-enantiomers of a novel, mechanism-based inhibitor, 2,3-diaminopropyl sulfate. Biochemistry 39:3091–3096

Dailey HA (2002) Terminal steps of haem biosynthesis. Biochem Soc Trans 30:590–595

Elder GH (1998) Update on enzyme and molecular defects in porphyria. Photodermatol Photoimmunol Photomed 14:66–69

Erskine PT, Senior N, Awan S, Lambert R, Lewis G, Tickle IJ, Sarwar M, Spencer P, Thomas P, Warren MJ, Shoolingin-Jordan PM, Wood SP, Cooper JB (1997) X-ray structure of 5-aminolaevulinate dehydratase, a hybrid aldolase. Nat Struct Biol 4:1025–1031

Erskine PT, Norton E, Cooper JB, Lambert R, Coker A, Lewis G, Spencer P, Sarwar M, Wood SP, Warren MJ, Shoolingin-Jordan PM (1999) X-ray structure of 5-aminolevulinic acid dehydratase from *Escherichia coli* complexed with the inhibitor levulinic acid at 2.0 Å resolution. Biochemistry 38:4266–4276

Frankenberg N, Lagarias JC (2003) Biosynthesis and biological functions of bilins. In: Kadish KM, Smith KM, Guilard R (eds) The porphyrin handbook. Elsevier, Amsterdam

Frankenberg N, Erskine PT, Cooper JB, Shoolingin-Jordan PM, Jahn D, Heinz DW (1999a) High resolution crystal structure of a Mg^{2+}-dependent porphobilinogen synthase. J Mol Biol 289:591–602

Frankenberg N, Jahn D, Jaffe EK (1999b) *Pseudomonas aeruginosa* contains a novel type V porphobilinogen synthase with no required catalytic metal ions. Biochemistry 38:13976–13982

Frere F, Schubert WD, Stauffer F, Frankenberg N, Neier R, Jahn D, Heinz DW (2002) Structure of porphobilinogen synthase from *Pseudomonas aeruginosa* in complex with 5-fluorolevulinic acid suggests a double Schiff base mechanism. J Mol Biol 320:237–247

Friedmann HC, Duban ME, Valasinas A, Frydman B (1992) The enantioselective participation of (S)- and (R)-diaminovaleric acids in the formation of delta-aminolevulinic acid in cyanobacteria. Biochem Biophys Res Commun 185:60–68

Fuchs J, Weber S, Kaufmann R (2000) Genotoxic potential of porphyrin type photosensitizers with particular emphasis on 5-aminolevulinic acid: implications for clinical photodynamic therapy. Free Radic Biol Med 28:537–548

Gibson KD, Laver WG, Neuberger A (1958) Initial steps in the biosynthesis of porphyrins. The formation of δ-aminolevulinic acid from glycine and succinyl-CoA by particles of chicken erythrocytes. Biochem J 70:71–81

Grimm B, Smith MA, von Wettstein D (1992) The role of Lys272 in the pyridoxal 5-phosphate active site of Synechococcus glutamate-1-semialdehyde aminotransferase. Eur J Biochem 206:579–585

Hadener A, Matzinger PK, Malashkevich VN, Louie GV, Wood SP, Oliver P, Alefounder PR, Pitt AR, Abell C, Battersby AR (1993) Purification, characterization, crystallisation and X-ray analysis of selenomethionine-labelled hydroxymethylbilane synthase from *Escherichia coli*. Eur J Biochem 211:615–624

Hadener A, Matzinger PK, Battersby AR, McSweeney S, Thompson AW, Hammersley AP, Harrop SJ, Cassetta A, Deacon A, Hunter WN, Nieh YP, Raftery J, Hunter N, Helliwell JR (1999) Determination of the structure of seleno-methionine-labelled hydroxymethylbilane synthase in its active form by multi-wavelength anomalous dispersion. Acta Crystallogr D Biol Crystallogr 55:631–643

Hansson M, Hederstedt L (1994) *Bacillus subtilis* HemY is a peripheral membrane protein essential for protoheme IX synthesis which can oxidize coproporphyrinogen III and protoporphyrinogen IX. J Bacteriol 176:5962–5970

Hennig M, Grimm B, Contestabile R, John RA, Jansonius JN (1997) Crystal structure of glutamate-1-semialdehyde aminomutase: an alpha2-dimeric vitamin B6-dependent enzyme with asymmetry in structure and active site reactivity. Proc Natl Acad Sci USA 94:4866–4871

Heurgue-Hamard V, Champ S, Engstrom A, Ehrenberg M, Buckingham RH (2002) The *hemK* gene in *Escherichia coli* encodes the N(5)-glutamine methyltransferase that modifies peptide release factors. EMBO J 21:769–778

Homuth G, Rompf A, Schumann W, Jahn D (1999) Transcriptional control of *Bacillus subtilis hemN* and *hemZ*. J Bacteriol 181:5922–5929

Hörtensteiner S (1999) Chlorophyll breakdown in higher plants and algae. Cell Mol Life Sci 56:330–347

Hunter GA, Ferreira GC (1999a) Lysine-313 of 5-aminolevulinate synthase acts as a general base during formation of the quinonoid reaction intermediates. Biochemistry 38:3711–3718

Hunter GA, Ferreira GC (1999b) Pre-steady-state reaction of 5-aminolevulinate synthase. Evidence for a rate-determining product release. J Biol Chem 274:12222–12228

Ilag LL, Jahn D (1992) Activity and spectroscopic properties of the *Escherichia coli* glutamate 1-semialdehyde aminotransferase and the putative active site mutant K265R. Biochemistry 31:7143–7151

Jaffe EK (2003) An unusual phylogenetic variation in the metal ion binding sites of porphobilinogen synthase. Chem Biol 10:25–34

Jahn D, Verkamp E, Söll D (1992) Glutamyl-transfer RNA: a precursor of heme and chlorophyll biosynthesis. Trends Biochem Sci 17:215–218

Jordan PM (1994) The biosynthesis of uroporphyrinogen III: mechanism of action of porphobilinogen deaminase. In: The biosynthesis of tetrapyrrole pigments. Wiley, Chichester

Jordan PM, Warren MJ (1987) Evidence for a dipyrromethane cofactor at the catalytic site of *E. coli* porphobilinogen deaminase. FEBS Lett 225:87–92

Kikuchi G, Kumar AM, Tamalge P, Shemin D (1958) The enzymatic synthesis of δ-aminolevulinic acid. J Biol Chem 233:1214–1219

Klemm DJ, Barton LL (1987) Purification and properties of protoporphyrinogen oxidase from an anaerobic bacterium, *Desulfovibrio gigas*. J Bacteriol 169:5209–5215

Laghai A, Jordan PM (1977) An exchange reaction catalysed by delta-aminolevulinate synthase from *Rhodopseudomonas spheroides*. Biochem Soc Trans 5:299–300

Layer G, Verfurth K, Mahlitz E, Jahn D (2002) Oxygen-independent coproporphyrinogen-III oxidase HemN from *Escherichia coli*. J Biol Chem 277:34136–34142

Lecerof D, Fodje M, Hansson A, Hansson M, Al-Karadaghi S (2000) Structural and mechanistic basis of porphyrin metallation by ferrochelatase. J Mol Biol 297:221–232

Lee HJ, Lee SB, Chung JS, Han SU, Han O, Guh JO, Jeon JS, An G, Back K (2000) Transgenic rice plants expressing a *Bacillus subtilis* protoporphyrinogen oxidase gene are resistant to diphenyl ether herbicide oxyfluorfen. Plant Cell Physiol 41:743–749

Luo J, Lim CK (1993) Order of uroporphyrinogen III decarboxylation on incubation of porphobilinogen and uroporphyrinogen III with erythrocyte uroporphyrinogen decarboxylase. Biochem J 289:529–532

Magnusson S, Ekstrom TJ, Elmer E, Kanje M, Ny L, Alm P (2000) Heme oxygenase-1, heme oxygenase-2 and biliverdin reductase in peripheral ganglia from rat, expression and plasticity. Neuroscience 95:821–829

Malik Z, Lugaci H (1987) Destruction of erythroleukaemic cells by photoactivation of endogenous porphyrins. Br J Cancer 56:589–595

Martens JH, Barg H, Warren MJ, Jahn D (2002) Microbial production of vitamin B_{12}. Appl Microbiol Biotechnol 58:275–285

Martins BM, Grimm B, Mock HP, Huber R, Messerschmidt A (2001) Crystal structure and substrate binding modeling of the uroporphyrinogen-III decarboxylase from *Nicotiana tabacum*. Implications for the catalytic mechanism. J Biol Chem 276:44108–44116

Mathews MA, Schubert HL, Whitby FG, Alexander KJ, Schadick K, Bergonia HA, Phillips JD, Hill CP (2001) Crystal structure of human uroporphyrinogen III synthase. EMBO J 20:5832–5839

Medlock AE, Dailey HA (1996) Human coproporphyrinogen oxidase is not a metalloprotein. J Biol Chem 271:32507–32510

Montforts FP, Glasenapp-Breiling M (2002) Naturally occurring cyclic tetrapyrroles. Fortschr Chem Org Naturst 84:1–51

Moser J, Lorenz S, Hubschwerlen C, Rompf A, Jahn D (1999) *Methanopyrus kandleri* glutamyl-tRNA reductase. J Biol Chem 274:30679–30685

Moser J, Schubert WD, Beier V, Bringemeier I, Jahn D, Heinz DW (2001) V-shaped structure of glutamyl-tRNA reductase, the first enzyme of tRNA-dependent tetrapyrrole biosynthesis. EMBO J 20:6583–6590

Moser J, Schubert WD, Heinz DW, Jahn D (2002) Structure and function of glutamyl-tRNA reductase involved in 5-aminolaevulinic acid formation. Biochem Soc Trans 30:579–584

Nandi DL (1978) Studies on delta-aminolevulinic acid synthase of *Rhodopseudomonas spheroides*. Reversibility of the reaction, kinetic, spectral, and other studies related to the mechanism of action. J Biol Chem 253:8872–8877

OBrian MR, Thöny-Meyer L (2002) Biochemistry, regulation and genomics of haem biosynthesis in prokaryotes. Adv Microb Physiol 46:257–318

ONeill GP, Söll D (1990) Transfer RNA and the formation of the heme and chlorophyll precursor, 5-aminolevulinic acid. Biofactors 2:227–235

Panek H, OBrian MR (2002) A whole genome view of prokaryotic haem biosynthesis. Microbiology 148:2273–2282

Raux E, Leech HK, Beck R, Schubert HL, Santander PJ, Roessner CA, Scott AI, Martens JH, Jahn D, Thermes C, Rambach A, Warren MJ (2003) Identification and functional analysis of enzymes required for precorrin-2 dehydrogenation and metal ion insertion in the biosynthesis of sirohaem and cobalamin in *Bacillus megaterium*. Biochem J 370:505–516

Sasarman A, Chartrand P, Lavoie M, Tardif D, Proschek R, Lapointe C (1979) Mapping of a new hem gene in *Escherichia coli* K12. J Gen Microbiol 113:297–303

Sasarman A, Letowski J, Czaika G, Ramirez V, Nead MA, Jacobs JM, Morais R (1993) Nucleotide sequence of the *hemG* gene involved in the protoporphyrinogen oxidase activity of *Escherichia coli* K12. Can J Microbiol 39:1155–1161

Schauer S, Chaturvedi S, Randau L, Moser J, Kitabatake M, Lorenz S, Verkamp E, Schubert WD, Nakayashiki T, Murai M, Wall K, Thomann HU, Heinz DW, Inokuchi H, Söll D, Jahn D (2002) *Escherichia coli* glutamyl-tRNA reductase. Trapping the thioester intermediate. J Biol Chem 277:48657–48663

Schauer S, Lüer C, Moser J (2003) Large scale production of biologically active *Escherichia coli* glutamyl-tRNA reductase from inclusion bodies. Protein Expr Purif (in press)

Schobert M, Jahn D (2002) Regulation of heme biosynthesis in non-phototrophic bacteria. J Mol Microbiol Biotechnol 4:287–294

Schubert HL, Raux E, Matthews MA, Phillips JD, Wilson KS, Hill CP, Warren MJ (2002a) Structural diversity in metal ion chelation and the structure of uroporphyrinogen III synthase. Biochem Soc Trans 30:595–600

Schubert W-D, Moser J, Schauer S, Heinz DW, Jahn D (2002b) Structure and function of glutamyl-tRNA reductase, the first enzyme of tetrapyrrole biosynthesis in plants and prokaryotes. Photosynth Res 74:205–215

Shemin D, Russell CS (1953) Delta-aminolevulinic acid, its role in the biosynthesis of porphyrins and purines. J Am Chem Soc 75:4873–4875

Shoolingin-Jordan PM, Spencer P, Sarwar M, Erskine PE, Cheung KM, Cooper JB, Norton EB (2002) 5-Aminolaevulinic acid dehydratase: metals, mutants and mechanism. Biochem Soc Trans 30:584–590

Shoolingin-Jordan PM, Al-Daihan S, Alexeev D, Baxter RL, Bottomley SS, Kahari ID, Roy I, Sarwar M, Sawyer L, Wang SF (2003) 5-Aminolevulinic acid synthase: mechanism, mutations and medicine. Biochim Biophys Acta 1647:361–366

Sidler W (1994) Phycobilisomes and phycobiliprotein structure. In: Bryant DA (ed) The molecular biology of cyanobacteria. Kluwer, Dordrecht, pp 139–216

Smith MA, Grimm B, Kannangara CG, von Wettstein D (1991a) Spectral kinetics of glutamate-1-semialdehyde aminomutase of Synechococcus. Proc Natl Acad Sci USA 88:9775–9779

Smith MA, Kannangara CG, Grimm B, von Wettstein D (1991b) Characterization of glutamate-1-semialdehyde aminotransferase of Synechococcus. Steady-state kinetic analysis. Eur J Biochem 202:749–757

Smith MA, Kannangara CG, Grimm B (1992) Glutamate 1-semialdehyde aminotransferase: anomalous enantiomeric reaction and enzyme mechanism. Biochemistry 31:11249–11254

Sofia HJ, Chen G, Hetzler BG, Reyes-Spindola JF, Miller NE (2001) Radical SAM, a novel protein superfamily linking unresolved steps in familiar biosynthetic pathways with radical mechanisms: functional characterization using new analysis and information visualization methods. Nucleic Acids Res 29:1097–1106

Thauer RK, Bonacker LG (1994) Biosynthesis of coenzyme F430, a nickel porphinoid involved in methanogenesis. Ciba Found Symp 180:210—227

Tyacke RJ, Contestabile R, Grimm B, Harwood JL, John RA (1995) Reactions of glutamate semialdehyde aminotransferase (glutamate-1-semialdehyde 2,1 aminomutase) with vinyl and acetylenic substrate analogues analysed by rapid scanning spectrophotometry. Biochem J 309:307–313

Vavilin DV, Vermaas WF (2002) Regulation of the tetrapyrrole biosynthetic pathway leading to heme and chlorophyll in plants and cyanobacteria. Physiol Plant 115:9–24

Verneuil H de, Sassa S, Kappas A (1983) Purification and properties of uroporphyrinogen decarboxylase from human erythrocytes. A single enzyme catalyzing the four sequential decarboxylations of uroporphyrinogens I and III. J Biol Chem 258:2454–2460

Warren MJ, Scott AI (1990) Tetrapyrrole assembly and modification into the ligands of biologically functional cofactors. Trends Biochem Sci 15:486–491

Weinstein JD, Beale SI (1983) Separate physiological roles and subcellular compartments for two tetrapyrrole biosynthetic pathways in *Euglena gracilis*. J Biol Chem 258:6799–6807

Whitby FG, Phillips JD, Kushner JP, Hill CP (1998) Crystal structure of human uroporphyrinogen decarboxylase. EMBO J 17:2463–2471

Wu CK, Dailey HA, Rose JP, Burden A, Sellers VM, Wang BC (2001) The 2.0 Å structure of human ferrochelatase, the terminal enzyme of heme biosynthesis. Nat Struct Biol 8:156–160

Zumft WG (1997) Cell biology and molecular basis of denitrification. Microbiol Mol Biol Rev 61:533–616